

RESEARCH

Open Access



Effects of riboflavin deficiency and high dietary fat on hepatic lipid accumulation: a synergetic action in the development of non-alcoholic fatty liver disease

Yanxian Wang¹, Xiangyu Bian¹, Min Wan¹, Weiyun Dong¹, Weina Gao¹, Zhanxin Yao¹ and Changjiang Guo^{1*}

Abstract

Background Non-alcoholic fatty liver disease (NAFLD) is characterized by excessive lipid accumulation in the liver. Riboflavin, one of water soluble vitamins, plays a role in lipid metabolism and antioxidant function. However, the effects of riboflavin deficiency on NAFLD development have not yet to be fully explored.

Methods In the present study, an animal model of NAFLD was induced by high fat diet feeding in mice and a cellular model of NAFLD was developed in HepG2 cells by palmitic acid (PA) exposure. The effects of riboflavin deficiency on lipid metabolism and antioxidant function were investigated both in vivo and in vitro. In addition, the possible role of peroxisome proliferator-activated receptor gamma (PPAR γ) was studied in HepG2 cells using gene silencing technique.

Results The results showed that riboflavin deficiency led to hepatic lipid accumulation in mice fed high fat diet. The expressions of fatty acid synthase (FAS) and carnitine palmitoyltransferase 1 (CPT1) were up-regulated, whereas that of adipose triglyceride lipase (ATGL) down-regulated. Similar changes in response to riboflavin deficiency were demonstrated in HepG2 cells treated with PA. Factorial analysis revealed a significant interaction between riboflavin deficiency and high dietary fat or PA load in the development of NAFLD. Hepatic PPAR γ expression was significantly upregulated in mice fed riboflavin deficient and high fat diet or in HepG2 cells treated with riboflavin deficiency and PA load. Knockdown of PPAR γ gene resulted in a significant reduction of lipid accumulation in HepG2 cells exposed to riboflavin deficiency and PA load.

Conclusions There is a synergetic action between riboflavin deficiency and high dietary fat on the development of NAFLD, in which PPAR γ may play an important role.

Keywords Riboflavin deficiency, Non-alcoholic fatty liver disease, Peroxisome proliferator-activated receptor gamma, Lipid metabolism, Oxidative stress

Introduction

Non-alcoholic fatty liver disease (NAFLD) refers to a pathological syndrome characterized by excessive intracellular fat deposition in the liver, including simple hepatic steatosis (SFL), nonalcoholic steatohepatitis (NASH), fibrosis, cirrhosis and related complications [1]. NAFLD has become one of the leading causes of

*Correspondence:

Changjiang Guo
guocjtj@126.com

¹ Institute of Environmental and Operational Medicine, Tianjin 300050, People's Republic of China



chronic liver diseases worldwide and is closely associated with obesity, type 2 diabetes mellitus and metabolic syndrome [2]. Globally, it was estimated that the prevalence of NAFLD was as high as 34.2% [3]. Despite its high prevalence, the pathogenesis of NAFLD is not clearly elucidated. The “two-hit” hypothesis proposed by Day and James suggested that impaired lipid metabolism is the first hit that leads to hepatic steatosis. The second hit comprises oxidative stress and lipid peroxidation, resulting in the development of NASH, fibrosis and cirrhosis [4]. Later, the “multiple hit” hypothesis was raised by Buzzetti et al., in which it was proposed that multiple insults (including insulin resistance, inflammatory cytokines, nutritional imbalance, gut microbiota, genetic and epigenetic factors) acted together in contributing to the development of NAFLD in genetically predisposed subjects [5]. Currently, it is recognized that impaired lipid metabolism plays an initial role in the pathogenesis of NAFLD [6, 7]. Peroxisome proliferator-activated receptor gamma (PPAR γ), a transcription factor that belongs to the family of PPARs nuclear receptors, is implicated in a wide range of biological processes, especially in regulating lipid metabolism [8–10]. Its expression was significantly upregulated in the liver of NAFLD mice and its knockdown led to attenuated hepatic lipid deposition [6–8], implying that it may play an important role in the development of NAFLD.

Numerous epidemiological and clinical studies have linked certain nutrients and dietary patterns to the occurrence of NAFLD [11–13]. The current data highlight the correlation between NAFLD and high intakes of saturated fat, red meats and fructose [14–16]. Riboflavin, a water-soluble vitamin, is mainly involved in energy metabolism in the forms of flavin mononucleotide (FMN) and flavin adenine dinucleotide (FAD). It also acts as a cofactor of glutathione reductase (GR) and is closely related to antioxidant function [17]. Recently, a dietary survey revealed that besides high dietary fat intake, insufficient riboflavin intake was prevalent in NASH patients [18]. Our previous rat experiment revealed that riboflavin deficiency led to a significant lipid accumulation in the liver [19]. Furthermore, a label-free proteomics study in HepG2 cells confirmed that riboflavin deficiency significantly affected NAFLD pathway based on KEGG pathway analysis [20], indicating that riboflavin deficiency may contribute to the development of NAFLD. Since riboflavin is an essential cofactor for several key enzymes in the lipid metabolism and antioxidant system, it is not surprising that riboflavin deficiency contributes to the pathogenesis of NAFLD, especially in the presence of high dietary fat intake. We hypothesize that riboflavin deficiency may synergize with high dietary fat to accelerate NAFLD development by compromising lipid metabolism

and antioxidant function. To test this hypothesis, we explored the effects of riboflavin deficiency on hepatic lipid accumulation and antioxidant function in mice fed a high-fat diet. An *in vitro* experiment was also carried out in HepG2 cells to validate the synergetic action of riboflavin deficiency and palmitic acid (PA) treatment on lipid accumulation and antioxidant function. The possible role played by PPAR γ was further investigated.

Materials and methods

Chemical reagents

Riboflavin (purity $\geq 99\%$), dimethyl sulfoxide (DMSO), bovine serum albumin (BSA) and PA were obtained from Sigma-Aldrich Co. (St. Louis, MO, USA). The stock solution of riboflavin (5 mM) was prepared in DMSO. PA was dissolved in a 100 mM sodium hydroxide solution by heating at 70 °C for 30 min and then mixed with 10% fatty acid-free BSA solution at 37 °C for 1 h, to yield a 5 mM PA solution [21]. Cell counting kit-8 (CCK8) and TRIzol RNA extraction reagents were purchased from Invitrogen (CA, USA). The protein quantification kit (BCA assay) and Oil red O staining kit were obtained from Beyotime Biotechnology Co., Shanghai, China. The assay kits for alanine aminotransferase (ALT), aspartate aminotransferase (AST), triglycerides (TG), total cholesterol (TC), glutathione reductase (GR), superoxide dismutase (SOD) and glutathione peroxidase (GSH-Px) were from Nanjing Jiancheng Bioengineering Institute, Nanjing, China. Fatty acid synthase (FAS), adipose triglyceride lipase (ATGL) and carnitine palmitoyltransferase 1 (CPT1) ELISA kits were from Jianglai Biotechnology Co., Shanghai, China. The primary antibodies used in this experiment were PPAR γ (Abcam, Cat# ab178860), glyceraldehyde-3-phosphate dehydrogenase (GAPDH) (Bioworld, Cat# MB001). The secondary antibodies were goat anti-mouse IgG (H&L)-HRP (Bioworld, Cat# BS12478) and goat anti-rabbit IgG (H&L)-HRP (Bioworld, Cat# BS13278).

Animal experiment

Animal experiment was carried out by following current Chinese legislation on the care and use of laboratory animals. The experimental protocol was approved by the Ethical Committee of the Department of Scientific Management of the institute. Thirty-six male 6–8 weeks old C57BL/6 mice (obtained from Huafukang Biotechnology Co., Beijing, China) were housed in a temperature (23–26 °C) and humidity (40–60%) controlled room with a 12 h light/dark cycle. After 1 week of adaptive feeding on a regular AIN-93 M diet, the animals were randomly divided into three groups. The control group (C) was continuously fed the regular AIN-93 diet. The high fat diet group (HFD) was switched to a high fat diet

containing 42% of energy from lard and 0.2% cholesterol [22], whereas the high fat and riboflavin deficient diet (HFRD) group to the high fat diet free of riboflavin, which was formulated according to the method of Bian et al. [19]. The compositions of the three diets were listed in Additional file 1: Tables S1–S3. The feeding period lasted 30 days. During the experiment, all mice had free access to water and food. Food intake was recorded daily, and body weight measured every 5 days. At the end of the experiment, mice were sacrificed under anesthesia via cervical dislocation. The blood collected from the orbital plexus was centrifuged to obtain serum. Liver tissues were harvested, fixed in 4% formalin at 4 °C for 24 h and then embedded in paraffin. Part of the liver samples were rapidly frozen in liquid nitrogen at –80 °C for biochemical assays, ELISA and Western blot analysis. The chart of experimental protocol was shown in Fig. 1.

Cell culture

Human hepatoma cell line HepG2 cells (purchased from Shanghai Institutes for Biological Sciences, Shanghai, China) were first grown to 60–80% confluence in Dulbecco's modified Eagle's medium (DMEM, Gibco) supplemented with 10% fetal bovine serum (FBS, Gibco) and antibiotics (100 U/mL penicillin and 100 mg/mL streptomycin) in an incubator (5% CO₂) at 37 °C. Then, they were divided into the normal control and experimental groups. The control cells were continuously cultured in the DMEM medium. The experimental cells were

transferred to the DMEM media (Basalmedia, Shanghai, China) formulated with different concentrations of riboflavin (0, 3, 12, 24 nM) in the presence or absence of PA. After cultured further for 96 h, cells were harvested and subjected to further analysis.

In our preliminary experiments, PA was selected to successfully induce lipid accumulation in HepG2 cells at the concentration of 10 μM without significantly influencing the viability of the cells. Therefore, the concentration of PA was set at 10 μM in this experiment. The concentrations of riboflavin in the medium were chosen based on the following reasons: 0 nM represents severe deficiency, which may occur in the plasma of premature infants treated with light therapy [23] and in cystic fibrosis patients with a severe deficiency [24]; 3 nM represents the level of riboflavin in the plasma of moderately deficient pregnant women [25]; 12 nM represents the riboflavin concentration in normal human plasma [26]; 24 nM represents a sufficient concentration of riboflavin in well-nourished human plasma [20].

Hematoxylin and eosin staining and NAFLD activity score of the liver

The liver sections were processed according to the standardized hematoxylin and eosin (H&E) staining procedure. The pathological changes were observed under a light microscope and analyzed using the NAFLD activity score (NAS) method developed by the International Pathology Committee [27].

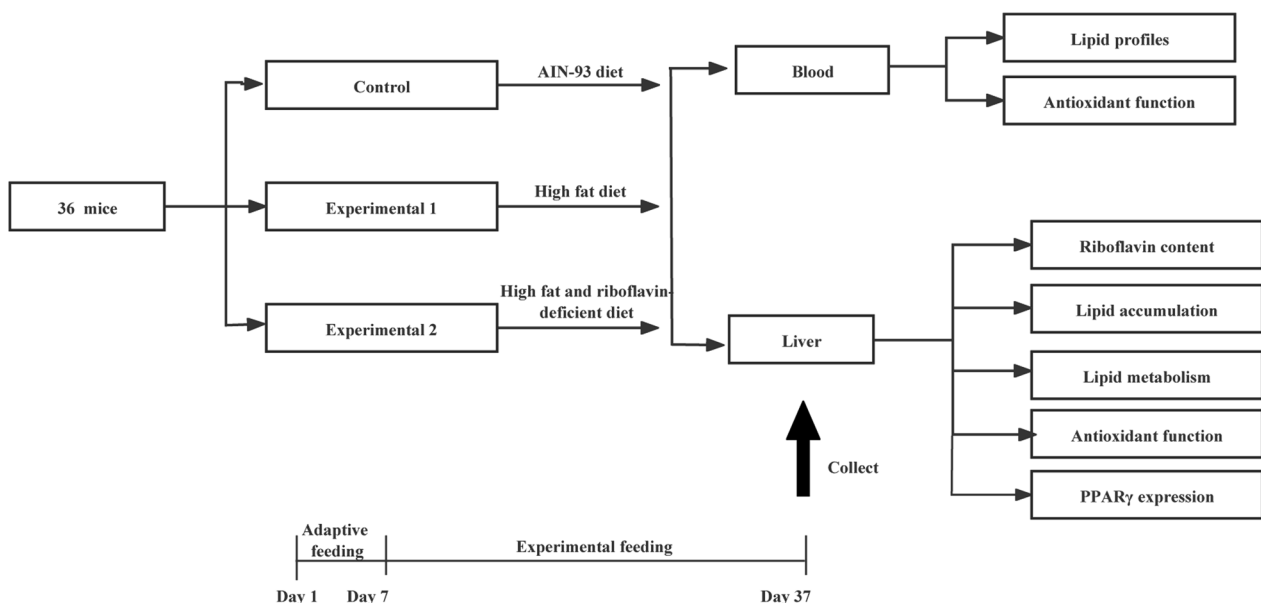


Fig. 1 The protocol of animal experiment. C57BL/6 were randomly divided into three groups, including control (C), high fat diet (HFD) and high fat and riboflavin deficient diet (HFRD) groups, and fed for 30 days. After the feeding period, serum and liver samples were collected for follow-up analysis

Cell viability assay

After cells were washed with PBS, 10 μ L CCK8 reagent was added and further incubated for 1 h at 37 °C with 5% CO₂. The absorbance was measured at 450 nm using a microplate reader (BioTek, USA). The manufacturer's instructions attached were strictly followed.

Oil red O staining

The liver tissues were fixed in 4% formalin and embedded in paraffin wax. Then, they were embedded in optimum cutting temperature compound and stained with Oil red O kit according to the manufacturer's instructions [28].

The HepG2 cell samples were washed twice with PBS and then fixed with 4% polyformaldehyde for 10 min. Oil red O staining is performed according to the manufacturer's instructions. After dyeing, the cells were washed twice with PBS and observed under light microscope. Finally, the Oil red O stained in the cells was dissolved in 500 μ L isopropanol, and 100 μ L of isopropanol from each well was transferred to a 96-well plate. The absorbance at 510 nm was measured using a microplate reader to qualify the accumulation of lipid drops.

Assessment of riboflavin status, liver function and lipid profiles

The contents of riboflavin, FMN and FAD in the liver were determined by a high performance liquid chromatography procedure described by Bian et al. [19]. The activities of ALT and AST in the serum, as well as the contents of TG and TC in the serum and liver were measured using the corresponding assay kits. All measurements were performed strictly in line with the instructions attached.

Measurement of GR, SOD and GSH-Px activities

Corresponding commercial assay kits were used to measure GR, SOD and GSH-Px activities in the liver, serum or cultured cells. The activities GR, SOD and GSH-Px in the liver and cultured cells were normalized by the protein content as determined by BCA assay.

Determination of ATGL, FAS and CPT1 levels

The protein levels of the enzymes involved in lipid metabolism in the liver and cultured cells, including ATGL, FAS and CPT1, were determined using corresponding commercial ELISA kits. All results were normalized by the protein content as determined by BCA assay.

Western blot analysis

Total protein extracts of the cell lysates were prepared using RIPA lysis buffer and denatured at 95 °C for

10 min. Then, they were separated on 12% SDS-PAGE and electrophoretically transferred onto a PVDF membrane (Merck Millipore, NJ, USA). The immunoreactive protein bands were visible after interaction with the primary antibodies, followed by incubation with the corresponding secondary antibodies. GAPDH was used as the reference protein. Densitometric analysis was performed using a chemiluminescence scanner (Amersham Pharmacia Biotech, Inc., USA), and the results were expressed as the ratio of the optical density of the target proteins to that of GAPDH.

Reverse transcription-polymerase chain reaction (RT-PCR) analysis

The mRNA expression of PPAR γ was measured by RT-PCR analysis. The primer was purchased from Sangon Biotech Co., Ltd (Shanghai, China). Total RNA was extracted from the cultured cells using Trizol reagent and quantified using a Nano Photometer (Thermo Scientific, MA, USA). PrimeScriptTM RT Master Mix (Takara, Beijing, China) was used to reverse-transcribe 400 ng of RNA into cDNA. The RT-PCR system consisted of 10 μ L TB Green Premix Ex Taq II (Takara, Beijing, China), 0.8 μ L upstream and downstream primers, 0.4 μ L ROX Reference Dye II (Takara, Beijing, China), 2 μ L template cDNA, and 6 μ L DEPC water (Takara, Beijing, China). The reaction conditions were 95 °C for 30 s, 40 cycles of 95 °C for 5 s and 60 °C for 30 s. The expression level of the PPAR γ gene was calculated by the 2^{- $\Delta\Delta$ Ct} method using the housekeeping gene 18S rRNA as the reference. The primer sequences are listed in Table 1.

Small interfering RNA (siRNA) transfection

Regarding RNA silencing, the siRNA sequence targeting human PPAR γ was designed and synthesized by Hanbio Technology Co., Ltd. (Shanghai, China). The specific sense and antisense strand sequences are shown in Table 2. HepG2 cells were transfected with 30 pmol siRNA for gene silencing using Lipofectamine RNAiMAX transfection reagent (Invitrogen, USA) according to the manufacturer's instructions. Six hours after transfection, the transfection efficiency was observed by fluorescence microscopy. In addition, RT-PCR and Western blot were used to evaluate the transfection efficiency at the end of the cell culture.

Table 1 Primer sequences used for RT-PCR analysis

	Forward primer (5'-3')	Reverse primer (5'-3')
PPAR γ	GTGAAGGGCAAGCCACTCTG	AGAGAGGGTCCCATTTCGGA
18S rRNA	CAGCCACCCGAGATTGAGCA	TAGTAGCGACGGCGGTGTG

Table 2 siRNA sequences for transfection

	Forward primer (5′–3′)	Reverse primer (5′–3′)
siRNA PPAR γ	AUGGAGUCCACGAGAUCAUUUTT	AAAUGAUCUCGUGGACUCCAUTT
siRNA Control	UUCUCCGACGUGUCACGUTT	ACGUGACACGUUCGGAGAATT

To investigate the role of PPAR γ in lipid metabolism of HepG2 cells treated with riboflavin deficiency combined with PA load, PPAR γ siRNA was transfected before being cultured in media containing 10 μ M PA or/and riboflavin deficiency for 96 h. Finally, cells were collected and subjected to further analysis.

Statistical analysis

All statistical analyzes were performed using SPSS version 21 software. Data are expressed as mean \pm standard deviation. Differences among groups were analyzed by one-way analysis of variance followed by Tukey's multiple comparison test. Factorial analysis was applied to analyze the interaction between riboflavin deficiency and PA load. $P < 0.05$ was considered significant statistically.

Results

Animal experiment

Riboflavin deficiency is developed in mice after feeding the high fat and riboflavin deficient diet

Compared to the C group, the HFD and HFRD groups consumed significantly less food during the experimental period (Fig. 2A). At the end of the experiment, body weight was significantly lower in the HFRD group than in the C and HFD groups (Fig. 2B). As shown in Fig. 2C–E, hepatic contents of riboflavin, FAD, and FMN in HFRD mice were significantly decreased by 70.8%, 43.2% and 47.15%, respectively in comparison with the C mice. However, there was no significant difference between the C and HFD groups. These results showed that riboflavin deficiency was successfully developed in HFRD mice.

Riboflavin deficiency further compromises lipid metabolism in mice fed the high fat diet

The liver index was remarkably increased in the HFD group compared to the C group. A more significant increase in the liver index were noted in the HFRD group (Fig. 3A). Meanwhile, serum activities of ALT and AST were significantly increased in the HFD group. Compared to the HFD group, a more significant increase in serum activities of ALT and AST were seen in the HFRD group (Fig. 3B–D), suggesting that riboflavin deficiency leads to a more severe liver damage in mice fed the high fat diet. In consistent with the changes in the liver index and serum activities of ALT and AST, similar changes were found in the liver and serum contents of TG and TC

in the HFRD group, indicating that lipid metabolism is disturbed more significantly in mice fed the high fat and riboflavin deficient diet.

Macroscopic examination revealed that the livers became swollen and dull yellow in color after high fat diet feeding (Fig. 3E). Histopathological examination after H&E staining found that high fat diet feeding led to steatosis and balloon-like lesions in the liver (Fig. 3F) and NAS was significantly increased. The results of Oil red O staining showed that the accumulation of hepatic lipid droplets was remarkably increased in the HFD group. These pathological changes were worsen by riboflavin deficiency, as demonstrated by more significantly increased steatosis, ballooning and NAS in the HFRD group (Fig. 3F–G).

The protein expressions of FAS, ATGL and CPT1, three critical enzymes in fatty acid synthesis, triglyceride hydrolysis, and fatty acid oxidation were detected in the liver using ELISA technique [29–31]. Compared to the C group, the expression of FAS in the liver of the HFD mice was significantly increased and further elevated by 22.5% in the liver of the HFRD mice (Fig. 4A). On the other hand, the expression of ATGL in the liver of the HFD mice was significantly decreased and further dropped by 18.3% in the liver of the HFRD mice (Fig. 4B). The content of CPT1 in the liver of HFD mice did not change significantly, while it was increased by 69.5% in the HFRD mice (Fig. 4C). These results showed that riboflavin deficiency resulted in increased fatty acid synthesis and decreased triglyceride hydrolysis in mice fed the high fat diet.

The expression of hepatic PPAR γ was significantly up-regulated in HFD mice and further elevated by 39.3% in HFRD mice (Fig. 4D), suggesting that PPAR γ may contribute to the development of NAFLD.

Riboflavin deficiency further impairs antioxidant function in mice fed the high fat diet

GR, SOD and GSH-Px play critical roles in the antioxidant defense system [32–34] and their activities in the serum and liver were determined in the current study. Serum activity of GR was significantly reduced in mice fed the high fat diet. Meanwhile, the activities of SOD, and GSH-Px in the liver were significantly decreased in the HFD mice (Fig. 5A–C). Riboflavin deficiency further declined the activities of serum GR, liver SOD and GSH-Px by 28.6%, 11.9%, and 24.7%, respectively, in mice fed

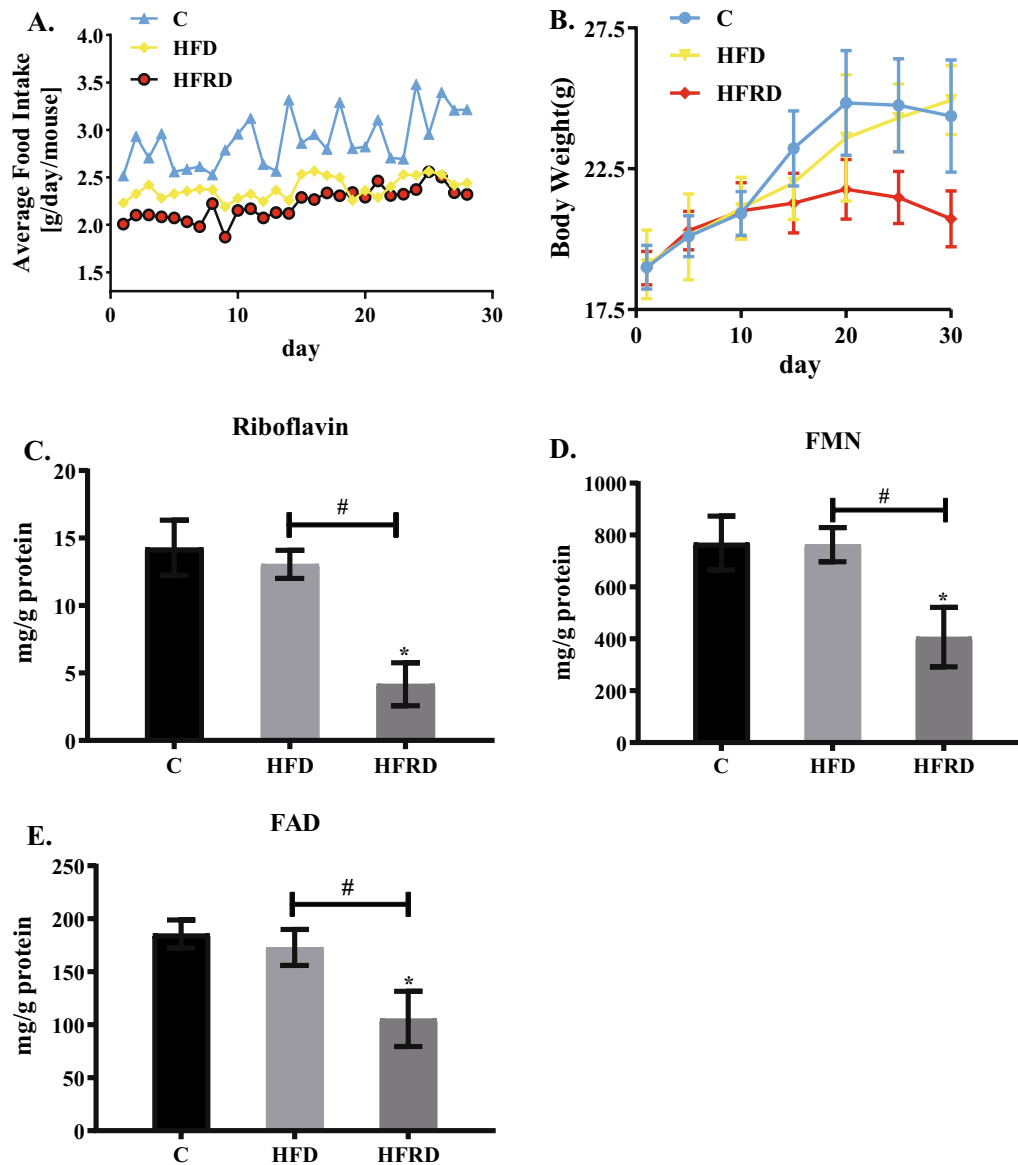


Fig. 2 Changes of riboflavin status after feeding different diets in mice. C57BL/6 mice were randomly divided into three groups, including control (C), high fat diet (HFD), high fat and riboflavin deficient diet (HFRD), and fed for 30 days. **A** Changes of daily food intake. **B** Changes of body weight. **C–E** The contents of riboflavin, FMN and FAD in the liver as determined by HPLC. Data are expressed as means \pm SD (n = 12). * $P < 0.05$ versus C; # $P < 0.05$ versus HFD

the high fat diet. These results indicate that riboflavin deficiency further impairs antioxidant function in the HFD mice.

Cell culture

Riboflavin deficiency and PA load synergistically alter lipid metabolism in HepG2 cells

As shown in Fig. 6A, it was confirmed that 10 μ M PA load did not significantly affect the viability of HepG2 cells. On the other hand, the viability of HepG2 cells was

significantly reduced when being cultured in media containing 0 or 3 nM riboflavin. Cell viability was normalized when the concentration of riboflavin in the medium was over 12 nM. However, no significant interaction between riboflavin and PA was found on the viability of HepG2 cells ($P > 0.05$) (Additional file 2: Table S1).

As shown by Oil red O staining, the accumulation of lipid droplets in HepG2 cells treated with riboflavin deficiency or PA was higher than that in the control group. More lipid droplet accumulation was noted when HepG2

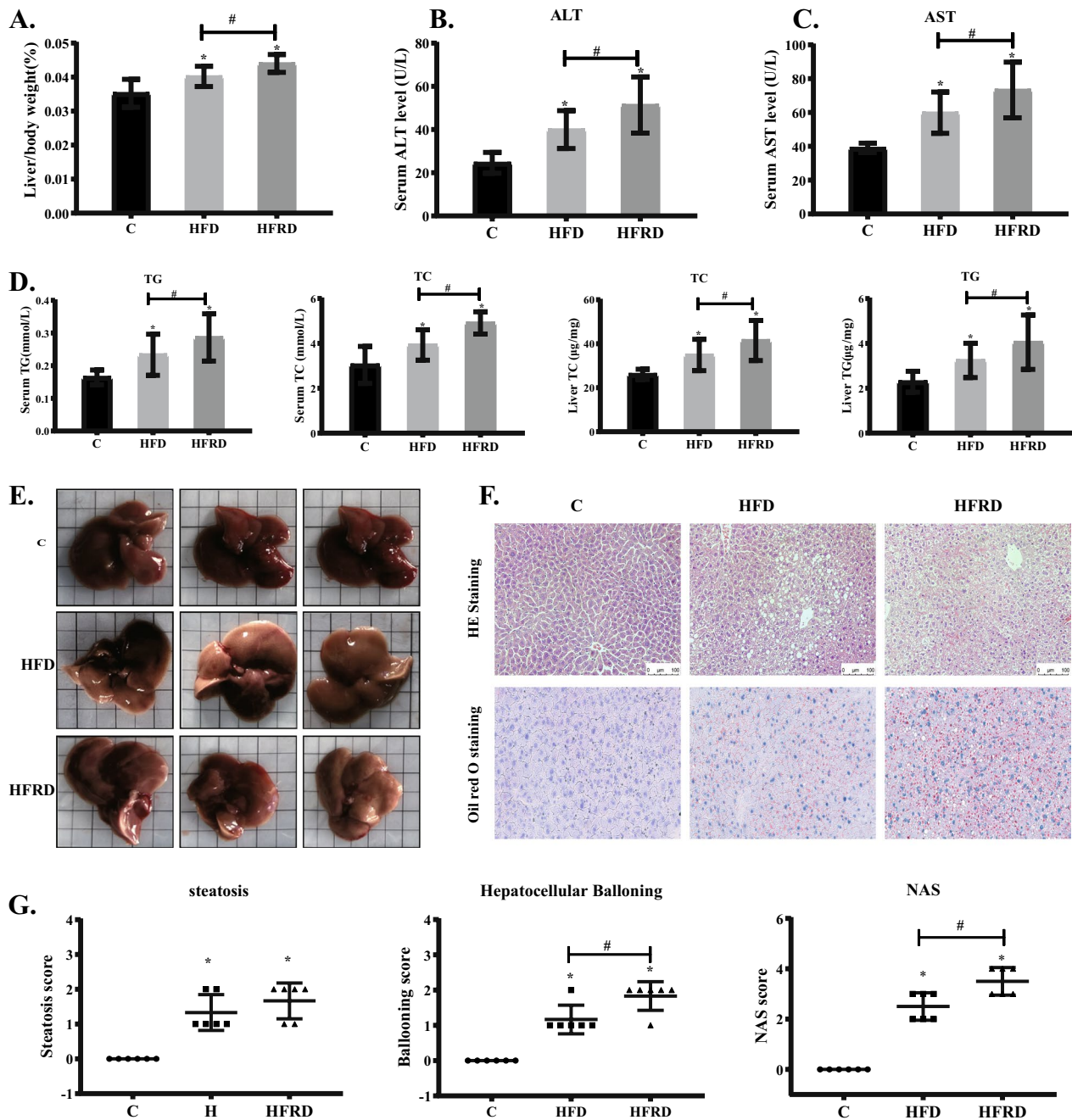


Fig. 3 Changes of liver index, histopathological structure and NAS after feeding different diets in mice. C57BL/6 mice were randomly divided into three groups, including control (C), high fat diet (HFD), high fat and riboflavin deficient diet (HFRD), and fed for 30 days. **A** Liver weight as a percentage of body weight. **B–C** Serum ALT and AST levels were determined using corresponding kits. **D** Serum and liver TG and TC levels were determined using corresponding kits. **E** Anatomical view of the liver. **F** Representative pictures of HE (20 \times) and Oil Red O (40 \times) stained liver sections. **G** NAFLD activity score, 6 mice per group. Data are expressed as means \pm SD. * $P < 0.05$ versus C; # $P < 0.05$ versus HFD

cells were treated with both riboflavin deficiency and PA load (Fig. 6B–C). The results of TG analysis also confirmed a significant increase in TG content in HepG2 cells after riboflavin deficiency or PA load compared to the control cells. More TG was detected in HepG2 cells

when being exposed to the combination of riboflavin deficiency and PA load (Fig. 6D). Factorial analysis confirmed a significant interaction between riboflavin deficiency and PA load on TG accumulation in HepG2 cells ($P < 0.05$) (Additional file 2: Tables S2–3).

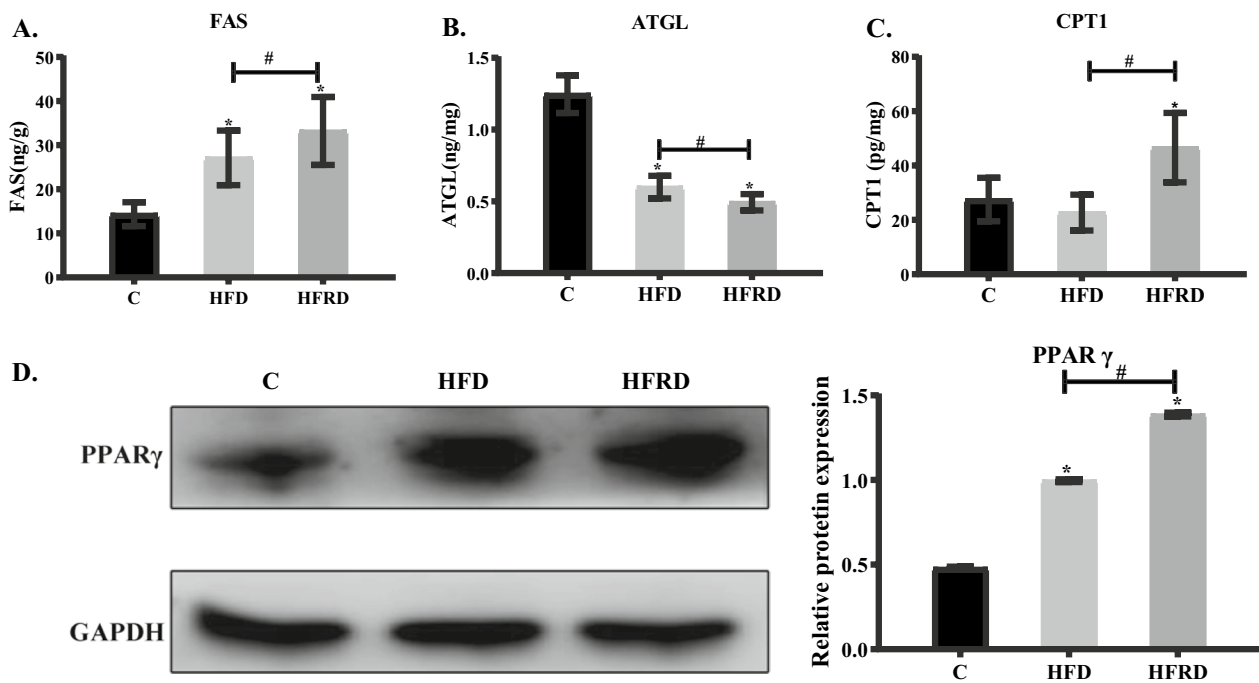


Fig. 4 Expressions of hepatic FAS, ATGL, CPT1 and PPAR γ after feeding different diets in mice. C57BL/6 mice were randomly divided into three groups, control (C), high fat diet (HFD), high fat and riboflavin deficient diet (HFRD), and fed for 30 days. **A–C** Liver FAS, ATGL and CPT1 contents were determined by the ELISA method. **D** Hepatic PPAR γ and GAPDH protein expressions were measured by Western blot analysis. The histogram is the grey value analysis of the corresponding protein bands. Data are expressed as means \pm SD ($n=3$). * $P < 0.05$ versus C; # $P < 0.05$ versus HFD

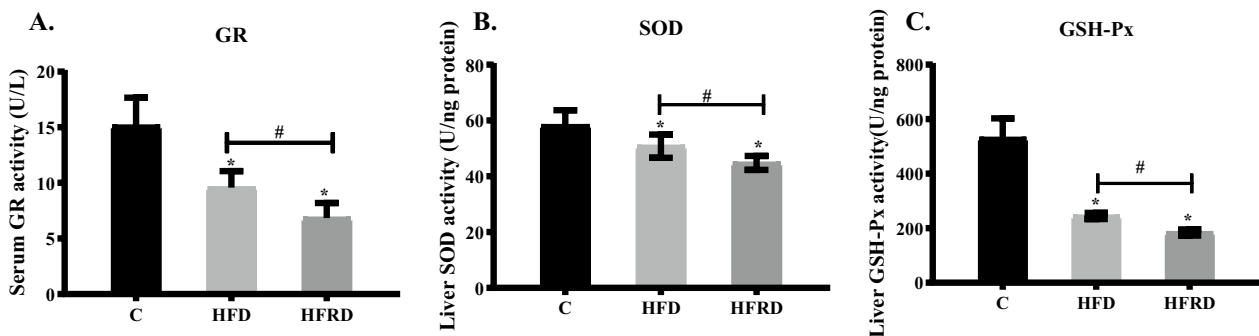


Fig. 5 Changes of serum GR, liver SOD and GSH-Px activities after feeding different diets in mice. C57BL/6 mice were randomly divided into three groups, including control (C), high fat diet (HFD), high fat and riboflavin deficient diet (HFRD), and fed for 30 days. The activities of serum SOD **A**, liver GR **B** and GSH-Px **C** were determined using corresponding kits. Data are expressed as means \pm SD ($n=12$). * $P < 0.05$ versus C; # $P < 0.05$ versus HFD

To explore the effects of riboflavin deficiency combined with PA load on the protein expression of the enzymes related to lipid metabolism, intracellular contents of FAS, ATGL and CPT1 were measured using ELISA technique. The protein expression of FAS was significantly increased in HepG2 cells treated with riboflavin deficiency or PA load compared to the control cells (Fig. 7A). When cells were cultured in media containing 0 nM or 3 nM riboflavin in the presence of PA, FAS

expression was further enhanced. A significant interaction occurred between riboflavin deficiency and PA load ($P < 0.05$) as shown by factorial analysis (Additional file 2: Table S4). As indicated in Fig. 7B, ATGL expression was significantly reduced in response to riboflavin deficiency or PA load compared to the control cells. ATGL expression was further declined when cells were cultured in media containing 0 nM or 3 nM riboflavin in the presence of PA. Factorial analysis demonstrated a

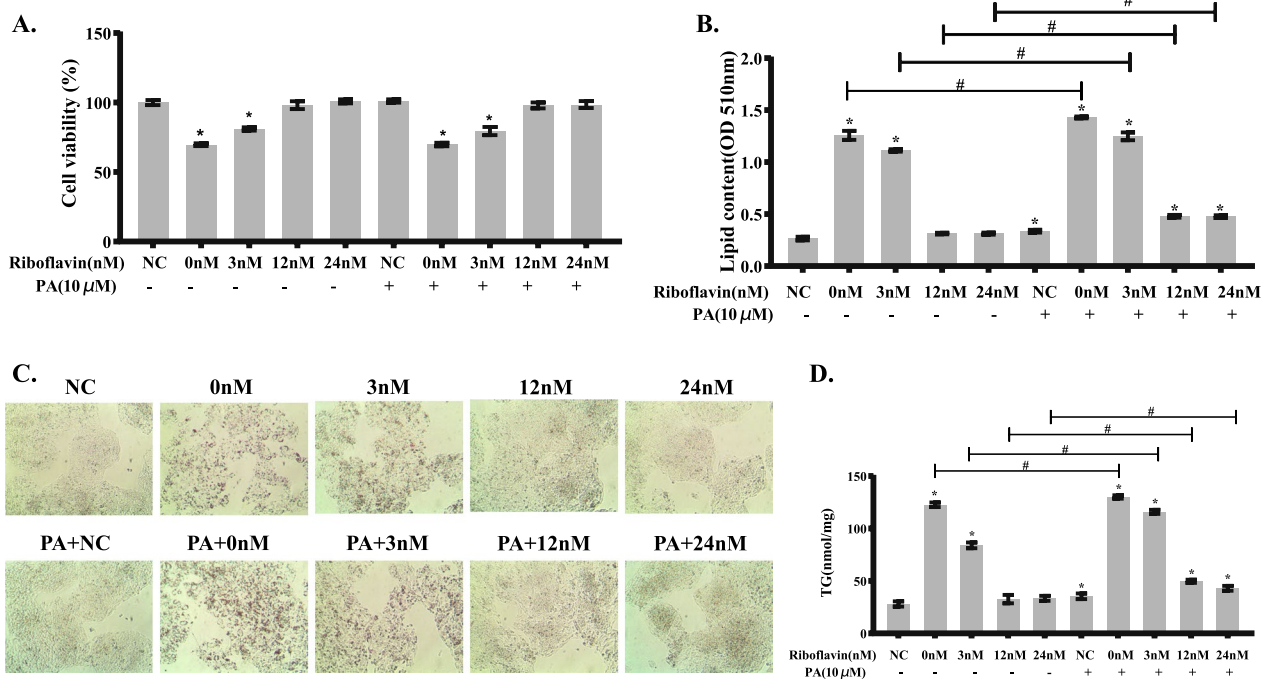


Fig. 6 Synergistic action between riboflavin deficiency and PA load in increasing lipid accumulation in HepG2 cells. The experimental cells were cultured in media containing various concentrations of riboflavin (0, 3, 12, 24 nM) in the presence or absence of PA (10 μM) for 96 h. **A** Cell viability was determined by CCK8 assay. **B** TG content in HepG2 cells was detected using commercial kit. **C** Oil red O staining of HepG2 cells (40× magnification). **D** Quantitative determination of TG accumulation in HepG2 cells by a colorimetric method. Data are shown as mean ± SD, and experiments were performed in triplicate. * $P < 0.05$ versus NC; Comparisons between various concentrations of riboflavin (0, 3, 12, 24 nM) in the presence of PA (10 μM) versus the absence of PA were statistically significant at # $P < 0.05$

synergistic action between riboflavin deficiency and PA load ($P < 0.05$) (Additional file 2: Table S5). PA load did not significantly affect the protein expression of CPT1 in HepG2 cells (Fig. 7C). However, riboflavin deficiency significantly increased the protein content of CPT1 at the concentration of 0 nM or 3 nM compared to the control cells. When cells were treated jointly with riboflavin deficiency and PA load, no further increase was noted in the intracellular CPT1 level. Factorial analysis did not demonstrate a significant interaction between riboflavin deficiency and PA load ($P > 0.05$) (Additional file 2: Table S6).

Riboflavin deficiency and PA load synergistically reduce antioxidant capacity in HepG2 cells

As indicated in Fig. 8A, GR activity was significantly lower in HepG2 cells treated with PA load or riboflavin deficiency than in the control cells. Although there was a further decline in GR activity in HepG2 cells when treated with PA load combined with riboflavin deficiency, the difference was not statistically significant. The activities of SOD and GSH-Px were also significantly reduced in riboflavin deficient or PA loaded cells. When treated with both PA load and riboflavin deficiency, the activities of SOD and GSH-Px were further significantly decreased

in HepG2 cells (Fig. 8B–C). There was a significant interaction between riboflavin deficiency and PA load on the activities of SOD and GSH-Px, as demonstrated by factorial analysis ($P < 0.05$) (Additional file 2: Tables S7–9). Taken together, riboflavin deficiency further impairs antioxidant function in PA loaded HepG2 cells.

Synergistic effects of riboflavin deficiency and PA load on lipid metabolism are partly reversed by PPAR γ gene silencing in HepG2 cells

To explore the possible mechanisms related to the synergistic action between riboflavin deficiency and PA load on lipid metabolism, we transfected HepG2 cells with PPAR γ siRNA and then cultured in PA loaded or/and riboflavin deficient media for 96 h. As seen in Fig. 9A–C, PPAR γ protein and mRNA expressions were significantly decreased in HepG2 cells after PPAR γ gene silencing, confirming a successful transfection. Meanwhile, lipid accumulation in the PA loaded cells was significantly decreased as evaluated by oil red O staining and TG assay (Fig. 9D–F). In the riboflavin deficient or riboflavin deficient and PA-loaded HepG2 cells, lipid droplet accumulation was significantly reduced after PPAR γ gene silencing as showed by Oil red O staining. TG content was also

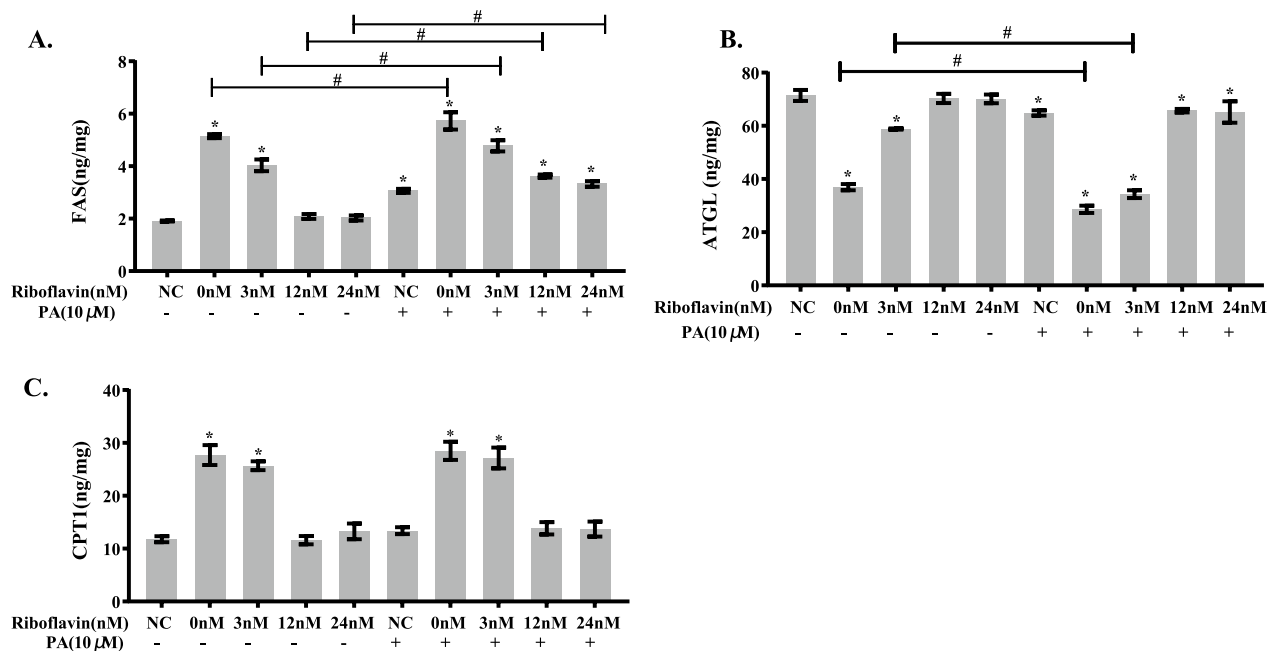


Fig. 7 Synergistic action between riboflavin deficiency and PA load in altering the expression of lipid metabolism related enzymes in HepG2 cells. HepG2 cells were cultured in media containing various concentrations of riboflavin (0, 3, 12, 24 nM) in the presence or absence of PA (10 μM) for 96 h. The protein levels of FAS (**A**), ATGL (**B**) and CPT1 (**C**) were analyzed by ELISA methods. Data are shown as mean ± SD, and experiments were performed in triplicate. * $P < 0.05$ versus NC; Comparisons between various concentrations of riboflavin (0, 3, 12, 24 nM) in the presence of PA (10 μM) versus the absence of PA were statistically significant at # $P < 0.05$

significantly lower in HepG2 cells treated with riboflavin deficiency or riboflavin deficiency combined with PA load after PPAR γ gene silencing by 230% and 284%, respectively as compared to the control cells. However, it did not recover completely to the normal level.

We further analyzed the changes of protein expressions of ATGL, FAS and CPT1 after PPAR γ siRNA transfection (Fig. 9G–I). The results showed that the content of FAS in HepG2 cells treated with PA load returned to the normal level after PPAR γ gene silencing. The expressions of FAS and CPT1 in HepG2 cells treated with riboflavin deficiency or riboflavin deficiency combined with PA load were also significantly lower after PPAR γ siRNA transfection. The expression of FAS in riboflavin deficient HepG2 cells was decreased by 39% and that in riboflavin deficient and PA loaded HepG2 cells decreased by 77% after PPAR γ silencing compared to the control cells. The expressions of CPT1 in HepG2 cells treated with riboflavin deficiency or riboflavin deficiency and PA load were decreased by 52% and 47%, respectively, after PPAR γ gene silencing. We also found that the level of ATGL, an enzyme involved in TG hydrolysis, was significantly decreased in HepG2 cells treated with PA load or/and riboflavin deficiency after PPAR γ silencing. These results indicate that the effects of riboflavin deficiency and PA load on lipid metabolism in HepG2 cells were alleviated

after PPAR γ gene silencing possibly by altering the expressions of the enzymes related to lipid metabolism.

Discussion

In the early stage, NAFLD manifests as increasing lipid accumulation in the liver. When the lipid content in the liver exceeds a certain threshold, hepatic steatosis will come into place [35, 36]. In this study, we utilized a diet-induced animal model of NAFLD, in which a high fat diet containing 42% of calories from fat and 0.2% of cholesterol was provided. It was showed that hepatic TG content was significantly increased after high fat diet feeding in mice, which is consistent with the data reported previously [37, 38]. FAS plays a critical role in hepatic lipogenesis and it was estimated that approximately 26% of the fat in the liver is from de novo lipogenesis in NAFLD patients [39]. In this study, the expression of hepatic FAS was significantly increased in the liver of HFD mice. ATGL, an enzyme response for TG hydrolysis [40, 41], was downregulated in expression in the liver of HFD mice. Meanwhile, antioxidant function was compromised as manifested by decreased activities of GR, SOD and GSH-Px. These data indicate that lipid metabolism, as well as the antioxidant defense system, is disturbed significantly by high fat diet feeding in mice and the animal model of NAFLD was successfully developed. The

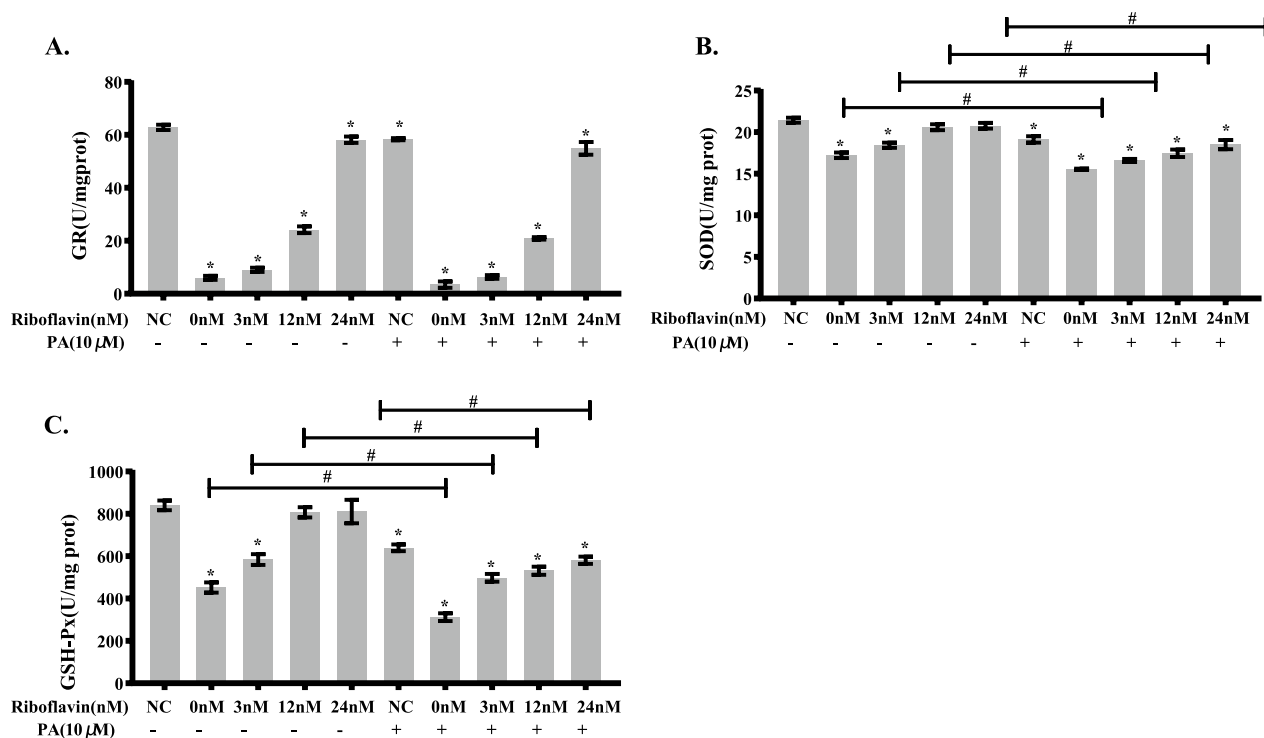


Fig. 8 Synergistic action between riboflavin deficiency and PA load in reducing the activities of antioxidant enzymes in HepG2 cells. HepG2 cells were cultured in media containing various concentrations of riboflavin (0, 3, 12, 24 nM) in the presence or absence of PA (10 μM) for 96 h. The activities of GR (A), SOD (B), and GSH-Px (C) in HepG2 cells were determined using corresponding kits. Data are shown as mean ± SD, and experiments were performed in triplicate. * $P < 0.05$ versus NC; Comparisons between various concentrations of riboflavin (0, 3, 12, 24 nM) in the presence of PA (10 μM) versus the absence of PA were statistically significant at # $P < 0.05$

present study provides evidence that riboflavin deficiency and high dietary fat act synergistically in disturbing lipid metabolism and antioxidant function. More lipid accumulation was found in the liver when mice were exposed to both riboflavin deficiency and high fat diet. The expressions of some enzymes related to lipid metabolism, including FAS, ATGL and CPT1, were also significantly altered. Meanwhile, the activities of serum GR, liver SOD and GSH-Px were reduced more significantly in mice exposed to both riboflavin deficiency and high dietary fat.

Since HepG2 cells retain most of the biochemical and morphological properties of human hepatocytes and have been applied extensively in studying hepatic lipid metabolism in association with NAFLD [42–44], a cellular model of NAFLD was successfully developed using PA load in HepG2 cells in this study to further investigate the interaction between riboflavin deficiency and PA load [21, 45]. Factorial analysis confirmed a significant interaction between riboflavin deficiency and PA load on TG content and the expressions of FAS, ATGL and CPT1 in HepG2 cells, which is basically in line with the data obtained from the animal experiment. It was also noted that riboflavin deficiency led to a more significant drop in

the activities of SOD and GSH-Px in PA exposed HepG2 cells.

PPAR γ is one of the nuclear receptors expressed in adipose tissue, and regulates the expression of genes related to glucose and lipid metabolism [46]. Activation of the PPAR γ gene in the liver increased de novo lipogenesis, and hepatocyte-specific PPAR γ gene knockdown was associated with decreased de novo lipogenesis [47–49]. Under normal conditions, PPAR γ expression is very low in the liver and increased with the development of hepatic steatosis in rodents and humans [7, 8, 50]. Currently, accumulated evidence supports the correlation between hepatic PPAR γ expression and NAFLD development [51, 52]. Interestingly, Hino et al. reported that riboflavin deficiency impaired the function of the mitochondrial electron transport chain and activated the expression of PPAR γ gene [53], implying that riboflavin deficiency may affect lipid metabolism by altering the expression of PPAR γ gene. Our study found that riboflavin deficiency increased the expression of PPAR γ in the liver of high fat diet fed mice. In vitro experiments also confirmed that the expression of PPAR γ in HepG2 cells treated with PA load combined with riboflavin deficiency was significantly higher compared to those treated with

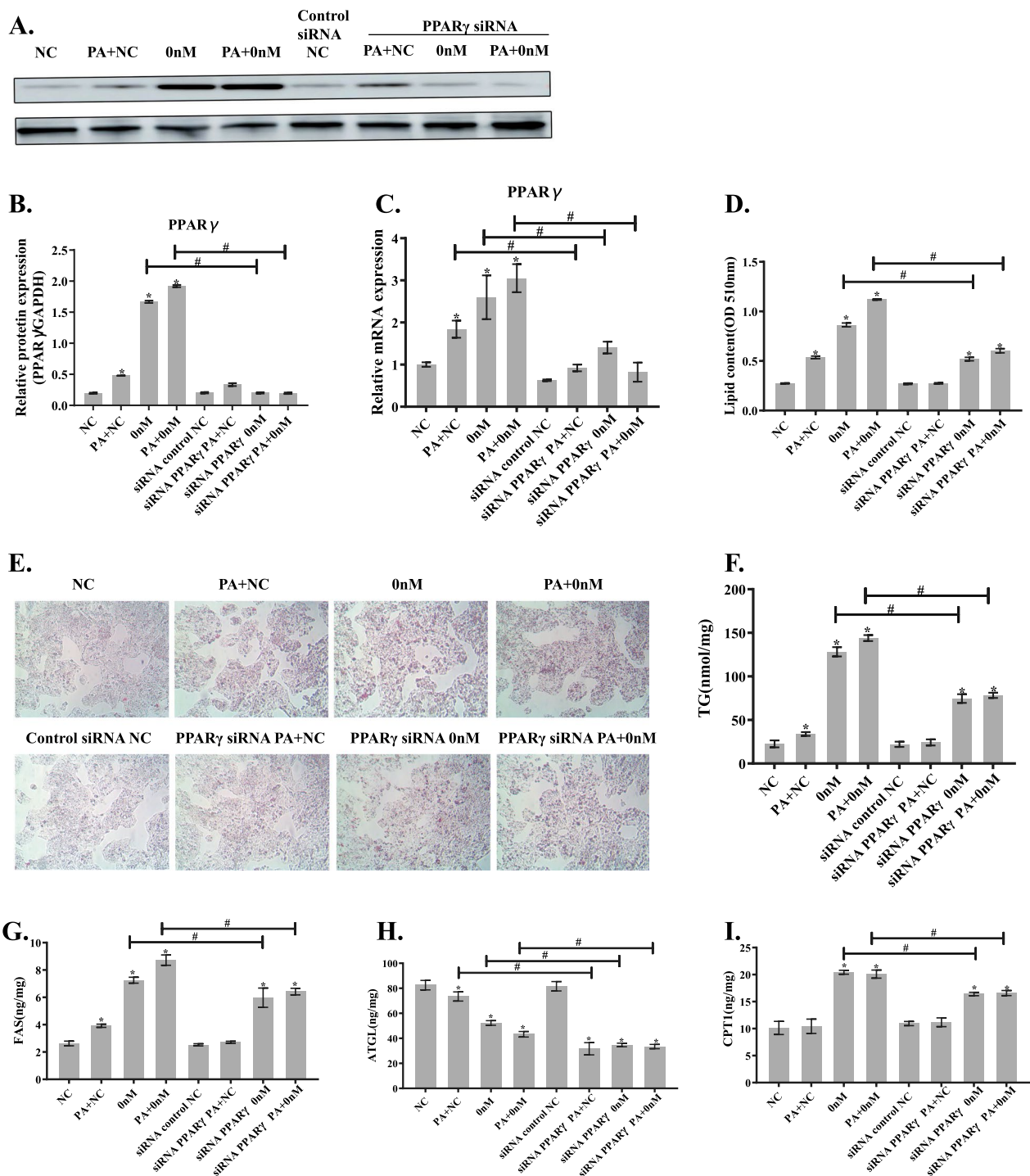


Fig. 9 PPAR γ gene silencing partly reverses disturbed lipid metabolism caused by riboflavin deficiency or/and PA load in HepG2 cells. HepG2 cells were cultured in the riboflavin free medium for 96 h in the presence or absence of PA (10 μ M) after blockade of PPAR γ expression with PPAR γ small interfering RNA (siRNA). **A** PPAR γ and GAPDH protein bands in HepG2 cells. **B** The histogram is the grey value analysis of the corresponding protein bands. **C** PPAR γ mRNA expression in HepG2 cells. **D** Quantitative determination of lipid droplets in HepG2 cells. **E** Oil red O staining of HepG2 cells (40x magnification). **F** TG content in HepG2 cells were detected using a commercial kit. The protein levels of FAS **G**, ATGL **H** and CPT1 **I** in HepG2 cells were analyzed by ELISA assay. * $P < 0.05$ versus NC; Comparisons before and after PPAR γ transfection were statistically significant at # $P < 0.05$

PA load or riboflavin deficiency alone. After silencing the expression of PPAR γ gene with corresponding siRNA, TG content was significantly decreased in HepG2 cells exposed to PA load or/and riboflavin deficiency. Furthermore, the expressions of FAS and CPT1 were changed toward to the normal. Therefore, PPAR γ may play an important role in the combined actions of riboflavin deficiency and high dietary fat in the development of NAFLD by normalizing the expressions of the lipid metabolism related enzymes.

Conclusions

We demonstrate for the first time that riboflavin deficiency and high dietary fat act synergistically to increase hepatic lipid accumulation both in vivo and in vitro, in which the PPAR γ pathway may be significantly involved. Our study provides experimental evidence in supporting the “multiple hit” hypothesis that multiple insults, including high dietary fat and riboflavin deficiency, are interacted in contributing to the development of NAFLD. Further intervention studies in NAFLD patients with riboflavin malnutrition are needed to be carried out to further confirm the interaction between riboflavin deficiency and high dietary fat.

Abbreviations

NAFLD	Non-alcoholic fatty liver disease
HFD	High-fat diet
PPAR γ	Peroxisome proliferator-activated receptor gamma
ATGL	Adipose triglyceride lipase
ACAD	Acyl CoA dehydrogenase
FAS	Fatty acid synthase
CPT1	Carnitine palmitoyltransferase 1
NASH	Nonalcoholic steatohepatitis
FMN	Flavin mononucleotide
FAD	Flavin adenine dinucleotide
GR	Glutathione reductase
PA	Palmitic acid
DMSO	Dimethyl sulfoxide
BSA	Bovine serum albumin
ALT	Alanine aminotransferase
AST	Aspartate aminotransferase
TG	Triglycerides
TC	Total cholesterol
SOD	Superoxide dismutase
GSH-Px	Glutathione peroxidase
C	Control
HFRD	High-fat riboflavin-deficient diet
ELISA	Enzyme immunoassay
NAS	NAFLD activity score
RT-PCR	Reverse transcription-polymerase chain reaction
siRNA	Small interfering RNA

Supplementary Information

The online version contains supplementary material available at <https://doi.org/10.1186/s12986-023-00775-8>.

Additional file 1. Feed composition in **Table S1** control, **Table S2** HFD and **Table S3** HFRD group.

Additional file 2. Factorial analysis of the synergistic effect of riboflavin deficiency and palmitic acid in **Table S1** Cells activity, **Table S2** Oil red O staining, **Table S3** Triglyceride Levels, **Table S4** FAS protein levels, **Table S5** ATGL protein levels, **Table S6** CPT1 protein levels, **Table S7** GR activity, **Table S8** GSH-Px activity, **Table S9** SOD activity.

Acknowledgements

The authors would like to thank the instrument support provided by the instrument platform of the Tianjin Institute of Environmental and Operational Medicine.

Author contributions

CG and YW conceived and designed the experiments, YW performed all of the experiments with assistance from XB, WG, and ZY; YW drafted the manuscript; CG provided funding; YW, MW, WD and CG wrote and revised the manuscript; All authors contributed to the article and approved the submitted version.

Funding

This study was supported by the National Natural Science Foundation of China [Grant No. 81973029].

Availability of data and materials

The datasets used and/or analyzed during the current study are available from the corresponding author on reasonable request.

Declarations

Ethics approval and consent to participate

During the experiment, the operation was strictly regulated to ensure the welfare of the experimental animals. All mice experiments mentioned in this present study were approved by the Institutional Animal Care and Use Committee of the Academy of Military Medical Sciences (approval number: 110322220103662617).

Consent for publication

Not applicable.

Competing interests

The authors have no conflict of interest to declare.

Received: 11 April 2023 Accepted: 19 December 2023

Published online: 02 January 2024

References

1. Tarantino G, Citro V, Capone D. Nonalcoholic fatty liver disease: a challenge from mechanisms to therapy. *J Clin Med*. 2020;9:15.
2. Riazi K, Azhari H, Charette JH, Underwood FE, King JA, Afshar EE, Swain MG, Congly SE, Kaplan GG, Shaheen A. The prevalence and incidence of NAFLD worldwide: a systematic review and meta-analysis. *Lancet Gastroenterol*. 2022;7:851–61.
3. Younossi ZM, Blissett D, Blissett R, Henry L, Stepanova M, Younossi Y, Racila A, Hunt S, Beckerman R. The economic and clinical burden of non-alcoholic fatty liver disease in the United States and Europe. *Hepatology*. 2016;64:1577–86.
4. Day CP, James OF. Steatohepatitis: A tale of two “hits”? *Gastroenterology*. 1998;114:842–5.
5. Buzzetti E, Pinzani M, Tsochatzis EA. The multiple-hit pathogenesis of non-alcoholic fatty liver disease (NAFLD). *Metabolism*. 2016;65:1038–48.
6. Issemann I, Green S. Activation of a member of the steroid hormone receptor superfamily by peroxisome proliferators. *Nature (London)*. 1990;347:645–50.
7. Jia X, Zhai T. Integrated analysis of multiple microarray studies to identify novel gene signatures in non-alcoholic fatty liver disease. *Front Endocrinol (Lausanne)*. 2019;10:599.

8. Gavrilova O, Haluzik M, Matsusue K, Cutson JJ, Johnson L, Dietz KR, Nicol CJ, Vinson C, Gonzalez FJ, Reitman ML. Liver peroxisome proliferator-activated receptor γ contributes to hepatic steatosis, triglyceride clearance, and regulation of body fat mass. *J Biol Chem*. 2003;278:34268–76.
9. Tontonoz P, Spiegelman BM. Fat and beyond: the diverse biology of PPAR γ . *Annu Rev Biochem*. 2008;77:289–312.
10. Ahmadian M, Suh JM, Hah N, Liddle C, Atkins AR, Downes M, Evans RM. PPAR γ signaling and metabolism: the good, the bad and the future. *Nat Med*. 2013;19:557–66.
11. Simpson SJE. The nutritional geometry of liver disease including non-alcoholic fatty liver disease (NAFLD). *J Hepatol*. 2018;68:316–25.
12. Mirizzi A, Franco I, Leone CM, Bonfiglio C, Cozzolongo R, Notarnicola M, Giannuzzi V, Tutino V, De Nunzio V, Bruno I, Buongiorno C, Campanella A, Defflorio V, Pascale A, Procino F, Sorino P, Osella AR. Effects of some food components on non-alcoholic fatty liver disease severity: results from a cross-sectional study. *Nutrients*. 2019;11:2744.
13. Saeed N, Nadeau B, Shannon C, Tincopa M. Evaluation of dietary approaches for the treatment of non-alcoholic fatty liver disease: a systematic review. *Nutrients*. 2019;11:3064.
14. Zelber-Sagi S, Ivancovsky-Wajcman D, Fliss Isakov N, Webb M, Orenstein D, Shibolet O, Kariv R. High red and processed meat consumption is associated with non-alcoholic fatty liver disease and insulin resistance. *J Hepatol*. 2018;68:1239–46.
15. Tsuchiya H, Ebata Y, Sakabe T, Hama S, Kogure K, Shiota G. High-fat, high-fructose diet induces hepatic iron overload via a hepcidin-independent mechanism prior to the onset of liver steatosis and insulin resistance in mice. *Metabolism*. 2013;62:62–9.
16. Rahman K, Desai C, Iyer SS, Thorn NE, Kumar P, Liu Y, Smith T, Neish AS, Li H, Tan S, Wu P, Liu X, Yu Y, Farris AB, Nusrat A, Parkos CA, Anania FA. Loss of junctional adhesion molecule 1 promotes severe steatohepatitis in mice on a diet high in saturated fat, fructose, and cholesterol. *Gastroenterology* (New York, NY 1943). 2016;151:733–46.
17. Pinto JT, Zemleni J. Riboflavin. *Adv Nutr*. 2016;7:973–5.
18. Federico A, Dallio M, Caprio G, Gravina A, Picascia D, Masarone M, Persico M, Loguercio C. Qualitative and quantitative evaluation of dietary intake in patients with non-alcoholic steatohepatitis. *Nutrients*. 2017;9:1074.
19. Bian X, Gao W, Wang Y, Yao Z, Xu Q, Guo C, Li B. Riboflavin deficiency affects lipid metabolism partly by reducing apolipoprotein B100 synthesis in rats. *J Nutr Biochem*. 2019;70:75–81.
20. Xin Z, Pu L, Gao W, Wang Y, Wei J, Shi T, Yao Z, Guo C. Riboflavin deficiency induces a significant change in proteomic profiles in HepG2 cells. *Sci Rep*. 2017;7:45861.
21. Joshi-Barve S, Barve SS, Amancherla K, Gobejishvili L, Hill D, Cave M, Hote P, McClain CJ. Palmitic acid induces production of proinflammatory cytokine interleukin-8 from hepatocytes. *Hepatology*. 2007;46:823–30.
22. Nanji AA. Animal models of nonalcoholic fatty liver disease and steatohepatitis. *Clin Liver Dis*. 2004;8:559–74.
23. Lucas A, Bates C. Transient riboflavin depletion in preterm infants. *Arch Dis Child*. 1984;59:837–41.
24. McCabe H. Riboflavin deficiency in cystic fibrosis: three case reports. *J Hum Nutr Diet*. 2001;14:365–70.
25. Manthey KC, Rodriguez-Melendez R, Hoi JT, Zemleni J. Riboflavin deficiency causes protein and DNA damage in HepG2 cells, triggering arrest in G1 phase of the cell cycle. *J Nutr Biochem*. 2006;17:250–6.
26. Manthey KC, Chew YC, Zemleni J. Riboflavin deficiency impairs oxidative folding and secretion of apolipoprotein B-100 in HepG2 cells, triggering stress response systems. *J Nutr*. 2005;135:978–82.
27. Brunt EM, Kleiner DE, Wilson LA, Belt P, Neuschwander-Tetri BA. Nonalcoholic fatty liver disease (NAFLD) activity score and the histopathologic diagnosis in NAFLD: distinct clinicopathologic meanings. *Hepatology*. 2011;53:810–20.
28. Sun Y, Xia M, Yan H, Han Y, Zhang F, Hu Z, Cui A, Ma F, Liu Z, Gong Q, Chen X, Gao J, Bian H, Tan Y, Li Y, Gao X. Berberine attenuates hepatic steatosis and enhances energy expenditure in mice by inducing autophagy and fibroblast growth factor 21. *Br J Pharmacol*. 2018;175:374–87.
29. Hu Y, He W, Huang Y, Xiang H, Guo J, Che Y, Cheng X, Hu F, Hu M, Ma T, Yu J, Tian H, Tian S, Ji YX, Zhang P, She ZG, Zhang XJ, Huang Z, Yang J, Li H. Fatty acid synthase-suppressor screening identifies sorting nexin 8 as a therapeutic target for NAFLD. *Hepatology*. 2021;74:2508–25.
30. Jha P, Claudel T, Baghdasaryan A, Mueller M, Halilbasic E, Das SK, Lass A, Zimmermann R, Zechner R, Hoefler G, Trauner M. Role of adipose triglyceride lipase (PNPLA2) in protection from hepatic inflammation in mouse models of steatohepatitis and endotoxemia. *Hepatology*. 2014;59:858–69.
31. Schlaepfer IR, Joshi M. CPT1A-mediated fat oxidation, mechanisms, and therapeutic potential. *Endocrinology*. 2020;161:bqz046.
32. Wang Y, Branicky R, Noë A, Hekimi S. Superoxide dismutases: dual roles in controlling ROS damage and regulating ROS signaling. *J Cell Biol*. 2018;21:1915–28.
33. Lai Y, Li M, Liao X, Zou L. Smartphone-assisted colorimetric detection of glutathione and glutathione reductase activity in human serum and mouse liver using hemin/G-quadruplex DNzyme. *Molecules*. 2021;26:5016.
34. Flohé L. Glutathione peroxidase. *Basic Life Sci*. 1988;49:663–8.
35. Masuoka HC, Chalasani N. Nonalcoholic fatty liver disease: an emerging threat to obese and diabetic individuals. *Ann NY Acad Sci*. 2013;1281:106–22.
36. Tanaka S, Hikita H, Tatsumi T, Sakamori R, Nozaki Y, Sakane S, Shiode Y, Nakabori T, Saito Y, Hiramatsu N, Tabata K, Kawabata T, Hamasaki M, Eguchi H, Nagano H, Yoshimori T, Takehara T. Rubicon inhibits autophagy and accelerates hepatocyte apoptosis and lipid accumulation in nonalcoholic fatty liver disease in mice. *Hepatology*. 2016;64:1994–2014.
37. Shi H, Prough RA, McClain CJ, Song M. Different types of dietary fat and fructose interactions result in distinct metabolic phenotypes in male mice. *J Nutr Biochem*. 2023;111:109189.
38. Lau JK, Zhang X, Yu J. Animal models of non-alcoholic fatty liver disease: current perspectives and recent advances. *J Pathol*. 2017;241:36–44.
39. Donnelly KL, Smith CI, Schwarzenberg SJ, Jessurun J, Boldt MD, Parks EJ. Sources of fatty acids stored in liver and secreted via lipoproteins in patients with nonalcoholic fatty liver disease. *J Clin Invest*. 2005;115:1343–51.
40. Brejchova K, Radner FPW, Balas L, Paluchova V, Cajka T, Chodounska H, Kudova E, Schratte M, Schreiber R, Durand T, Zechner R, Kuda O. Distinct roles of adipose triglyceride lipase and hormone-sensitive lipase in the catabolism of triacylglycerol estolides. *P Natl Acad Sci USA*. 2021;118:e202099918.
41. Chen Y, Jiang H, Zhan Z, Lu J, Gu T, Yu P, Liang W, Zhang X, Liu S, Bi H, Zhong S, Tang L. Restoration of lipid homeostasis between TG and PE by the LXR α -ATGL/EPT1 axis ameliorates hepatohepatosteatosis. *Cell Death Dis*. 2023;14:85.
42. Gomez-Lechon MJ, Donato MT, Martinez-Romero A, Jimenez N, Castell JV, O'Connor JE. A human hepatocellular in vitro model to investigate steatosis. *Chem Biol Interact*. 2007;165:106–16.
43. Cui W, Chen SL, Hu KQ. Quantification and mechanisms of oleic acid-induced steatosis in HepG2 cells. *Am J Transl Res*. 2010;2:95–104.
44. Ganji SH, Kashyap ML, Kamanna VS. Niacin inhibits fat accumulation, oxidative stress, and inflammatory cytokine IL-8 in cultured hepatocytes: impact on non-alcoholic fatty liver disease. *Metabolism*. 2015;64:982–90.
45. García-Ruiz I, Solís-Muñoz P, Fernández-Moreira D, Muñoz-Yagüe T, Solís-Herruzo JA. In vitro treatment of HepG2 cells with saturated fatty acids reproduces mitochondrial dysfunction found in nonalcoholic steatohepatitis. *Dis Model Mech*. 2015;8:183–91.
46. Tao H, Aakula S, Abumrad NN, Hajri T. Peroxisome proliferator-activated receptor- γ regulates the expression and function of very-low-density lipoprotein receptor. *Am J Physiol Endocrinol Metab*. 2010;298:E68–79.
47. Morán-Salvador EEA. Role for PPAR γ in obesity-induced hepatic steatosis as determined by hepatocyte- and macrophage-specific conditional knockouts. *FASEB J*. 2011;8:2538–50.
48. Silva AKS, Peixoto CA. Role of peroxisome proliferator-activated receptors in non-alcoholic fatty liver disease inflammation. *Cell Mol Life Sci*. 2018;16:2951–61.
49. Lambert JE, Ramos Roman MA, Browning JD, Parks EJ. Increased de novo lipogenesis is a distinct characteristic of individuals with nonalcoholic fatty liver disease. *Gastroenterology*. 2014;146:726–35.
50. Nakamura M, Kohjima M, Morizono S, Kotoh K, Yoshimoto T, Miyagi I, Enjoji M. Evaluation of fatty acid metabolism-related gene expression in nonalcoholic fatty liver disease. *Int J Mol Med*. 2005;16:631.
51. Pettinelli P, Videla LA. Up-regulation of PPAR- γ mRNA expression in the liver of obese patients: an additional reinforcing lipogenic mechanism to SREBP-1c induction. *J Clin Endocr Metab*. 2011;96:1424–30.
52. Lee SM, Muratalla J, Karimi S, Diaz-Ruiz A, Frutos MD, Guzman G, Ramos-Molina B, Cordoba-Chacon J. Hepatocyte PPAR γ contributes to the

progression of non-alcoholic steatohepatitis in male and female obese mice. *Cell Mol Life Sci.* 2023;80:39.

53. Hino S, Sakamoto A, Nagaoka K, Anan K, Wang Y, Mimasu S, Umehara T, Yokoyama S, Kosai K, Nakao M. FAD-dependent lysine-specific demethylase-1 regulates cellular energy expenditure. *Nat Commun.* 2012;3:758.

Publisher's Note

Springer Nature remains neutral with regard to jurisdictional claims in published maps and institutional affiliations.

Ready to submit your research? Choose BMC and benefit from:

- fast, convenient online submission
- thorough peer review by experienced researchers in your field
- rapid publication on acceptance
- support for research data, including large and complex data types
- gold Open Access which fosters wider collaboration and increased citations
- maximum visibility for your research: over 100M website views per year

At BMC, research is always in progress.

Learn more biomedcentral.com/submissions

